STAR NOTE #305
September 19, 1997

Simulation Study of γ/π^0– and e/h–Separation Powers in the STAR Barrel Electromagnetic Calorimeter with the Gaseous Shower Maximum Detector

A. A. Derevschikov, Yu. A. Matulenko,
K. E. Shestermanov,
A. N. Vasiliev, L. V. Alekseeva[1], L. V. Nogach[1]

Institute of High Energy Physics, Protvino, Russia

V. L. Rykov

Wayne State University, Detroit, MI 48202, USA

Abstract

The γ/π^o-separation has been studied using a gaseous Shower Maximum Detector (SMD) positioned at four different locations inside the STAR Electromagnetic Calorimeter (EMC), $3X_o$, $4X_o$, $5X_o$ and $7X_o$, for various energies of the incident particles in the range from 3 to 25 GeV.

Also an electron–hadron separation power of the STAR EMC with the gaseous SMD has been evaluated for two SMD positions within the EMC stack at the energies from 2 to 30 GeV.

[1]Graduate student from Moscow State University.

1 Introduction

In this Note, we provide the estimates for how well the STAR Barrel Electromagnetic Calorimeter (EMC) with the gaseous Shower Maximum Detector (SMD) can distinguish single photons from double-photon hits originated from π^0-decays which are the main background for the study of direct photon production and asymmetries. The similar study for the scintillator-strip/fiber SMD has been accomplished earlier and published in Ref. [1].

We have also estimated the EMC/SMD hadron rejection power for e/π-separation in the energy range from 2 to 30 GeV which is important for the both, Heavy-Ion and Spin Physics programs in STAR at RHIC.

The STAR is one of two large RHIC's detectors which, along with its rich capabilities for Heavy Ion Physics, will also carry out practically the entire Spin Program with polarized protons colliding at RHIC. Particularly, as it has been suggested in the RHIC Spin Proposal [2], the information on spin-dependent gluon structure functions will be obtained by measuring the asymmetries of direct photons and jet production at $P_T \geq 10$ GeV/c as well as by studying the production and decay asymmetries (including parity violation) for $W^\pm \to e^\pm \nu$ and $Z^0 \to e^+e^-$.

Single photons and dileptons are also regarded as the "penetrating" probes for Quark-Gluon Plasma (QGP) because they are produced at the early stage of the collision and are not affected by the subsequent hadronization of the system [3]. However, the region of interest here is at much lower $P_T \simeq 1$–7 GeV/c compared to polarized proton collisions. This, along with the much higher multiplicity of heavy-ion events, makes the task even more challenging.

At the stage of simulations presented here, we don't take into account the complications arising from the high multiplicity. We fully understand however that, because of this simplification, our estimates for γ/π^o-separation at low P_T can be considered as a rather very "remote scouting" the problem than its direct attack.

As it has been suggested in Ref. [4], the recognition of direct photons at $P_T \geq 7$–10 GeV/c is also interesting for the exploration of Jet Quenching mechanism in heavy ion collisions. The quantitative information about this phenomenon can be obtained by measuring the high-P_T hadron spectra in the events tagged with the high-P_T direct photons. The problem of high multiplicity of heavy ion collisions seems, to some extent, less significant here than at lower P_T's. However, this data are not expected to be among the first results from Au-Au collisions at RHIC since a quite high integrated luminosity is required for the accumulation of a statistically sufficient sample of events.

The results presented below have been obtained, using GEANT–3.21 code. The GEANT parameters for simulating the electromagnetic showers in the EMC/SMD have been chosen, following the recommendation of Ref. [5]: ISTRA = 1, ILOSS = 1; with the thresholds of

– 500 keV for electrons/positrons in Pb and Scintillator material;

– 80 keV for γ-quanta in Pb and Sc;

– 10 keV for $e^{\pm}$ and γ in the gaseous SMD.

To simulate the hadron showers, GHEISHA code have been used.

Usually, a sample of 500 events have been generated at each SMD position in the EMC stack for each energy.

It should be noticed that, in these simulations, the energy depositions in active media (scintillator layers and SMD gas mixture) and their fluctuations only have been taken into account. All other effects (statistics of photoelectrons in the EMC, charge collection in the SMD, EMC and SMD segmentations, edge effects, etc) have been ignored which is apparently one more major simplification of this stage simulations. We suppose to include these effects at the next stage along with the GEANT parameters better "tuned up" to the EMC/SMD test beam data which are available now.

2 The Geometry of the Electromagnetic Calorimeter and Shower Maximum Detector

The EMC geometry used in these simulations was the non-segmented block of Scintillator-Lead calorimeter with the cross-section 70×70 cm^2 and with the gaseous SMD placed inside the stack. The calorimeter stack consisted of 20 sandwich-type layers of the thickness approximately equal to 0.9 of radiation length (X_o) each. In turn, each layer consisted of 4 mm thick scintillator tile plus 1.3 mm $G10$ plate plus 5 mm thick Pb plate. The 19 mm thick Aluminum plate has been placed in front of the stack, exactly as it's supposed to be in the real STAR EMC.

In our simulations, the "CDF-type" [6] SMD placed after the 3d –7th EMC layer, was actually the multi-wire proportional chamber enclosed into the Aluminum flat box with the 2 mm thick front plate and 4 mm thick back plate. Just behind the front plate, the 4 mm thick G10 printed circuit board with the cathode strips at its surface has been placed. The 6 mm thick ionization sensitive volume between this board and Al back plate was filled with the 70% Ar plus 30% CO_2 gas mixture.

The readout from SMD in Y-direction was from the anode wires separated from each other by 7 mm. The readout in the orthogonal, X-direction, was from 14 mm wide signal cathode strips[1].

The initial particles from the source (γ, electrons, and π-mesons) have been directed toward the EMC block central area of the size $10 \times 10\,cm^2$, perpendicularly to its front plate. The source of incident particles has been located at the 220 cm distance from the EMC front plate.

3 SMD Characteristics

In 1995, the IHEP-built gaseous SMD prototype had been tested at the AGS test beam in the energy range from ∼1 to 7 GeV [7]. This SMD had been positioned in the Small EMC prototype (SPEMC) at the depth of $\sim 5X_o$. The beam Čerenkov counter has been used to select electrons among others negative particles, mainly π^-'s, striking SPEMC. In Fig.1, an electron shower shape in the SMD simulated with GEANT is compared to the experimental one. Their reasonably good agreement can be observed.

The experimental shape has been obtained [8] using two hodoscopes in front of SPEMC for measuring X- and Y-positions with 2-mm wide scintillator rods. Therefore, the experimental shower profile in Fig.1 is actually smeared with the 2-mm hodoscope resolution. The GEANT simulated

[1] In the STAR EMC project, it has been suggested the anode wires to be paired for having about equal, ∼14-15 mm, segmentations in both directions. In this simulations, however, we followed the design of the SMD prototype as of 1995 where each anode wire represented a separate readout channel.

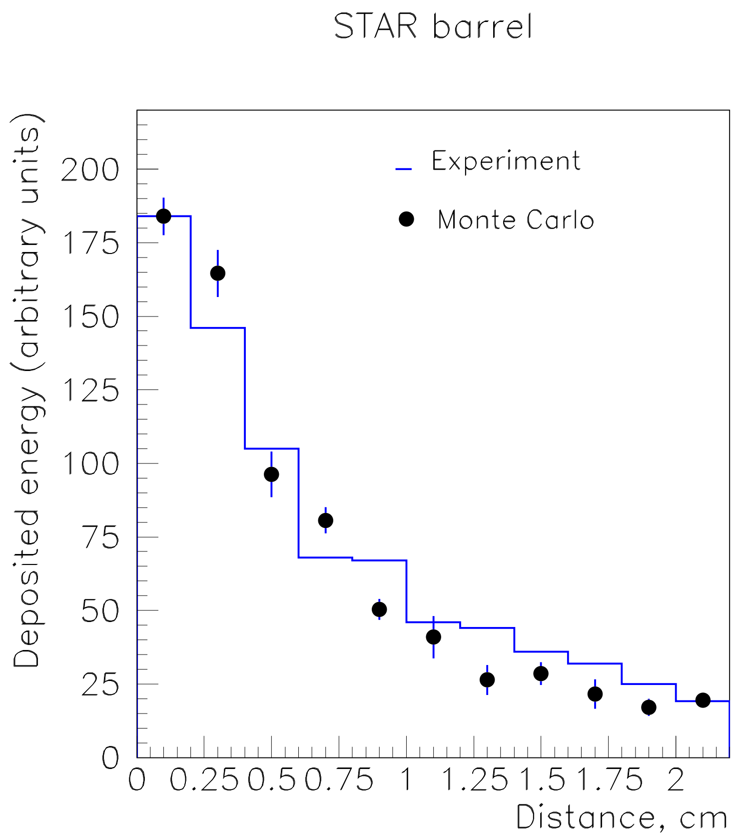

Figure 1: Experimental and Monte-Carlo shower shapes in the SMD located after $5X_o$ within the EMC. Incident particles are 5 GeV electrons.

shower shape for 5 GeV electrons has been produced in the similar way with the same smearing which was actually achieved by 2-mm wide binning of the accumulated histogram for energy deposition in the SMD gas. For normalization, two profiles in Fig.1 have been equalized in their first bins.

Fig.2 shows the mean energy deposition in the SMD sensitive volume versus the energy of incident photons, for various SMD locations within the EMC. The energy deposited in the SMD is very small, on the order of $\approx 10^{-5}$ of the energy of incident photons or electrons. For the deep SMD position at $7X_o$, its response is quite linear up to $\sim$15–20 GeV while at more shallow locations, the noticeable non-linearity shows up earlier.

The GEANT simulated position resolutions in the SMD for γ-quanta are

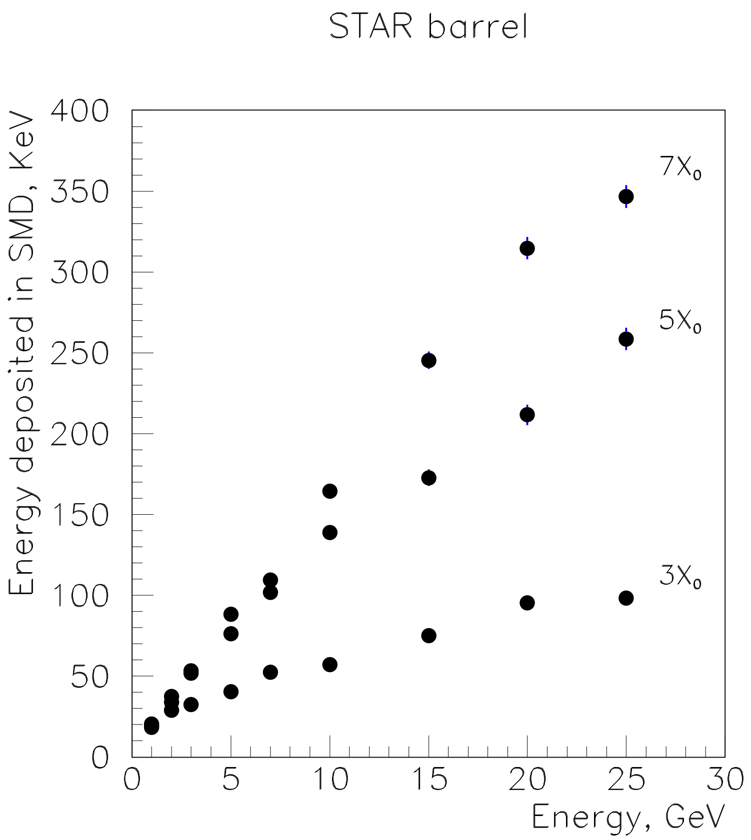

Figure 2: Energy deposition in the SMD versus energy of incident photons for three SMD locations inside the EMC: $3X_o$, $5X_o$ and $7X_o$.

shown in Fig.3. In this figure, the characteristic σ is actually the "sigma" of the Gaussian fit to the distributions of differences between the "true" hit position and the "logarithmic weighted center of shower". For the "true" hit position, the crossing point of the trajectory of incident photon with the SMD mid-plane has been chosen. The coordinates of the "logarithmic weighted center of shower" in the SMD, X_c and Y_c, have been calculated, using the formulae [9]:

$$X_c = \frac{\sum_i X_i W_i}{\sum_i W_i}; \quad Y_c = \frac{\sum_i Y_i W_i}{\sum_i W_i} \quad \text{with} \quad W_i = max\{0, W_0 + ln(E_i/E_{tot})\} \quad (1)$$

In the formulae above, E_i is the energy deposited under the i-th cathode strip or in the i-th wire's cell; X_i is the position of the center line of the i-th

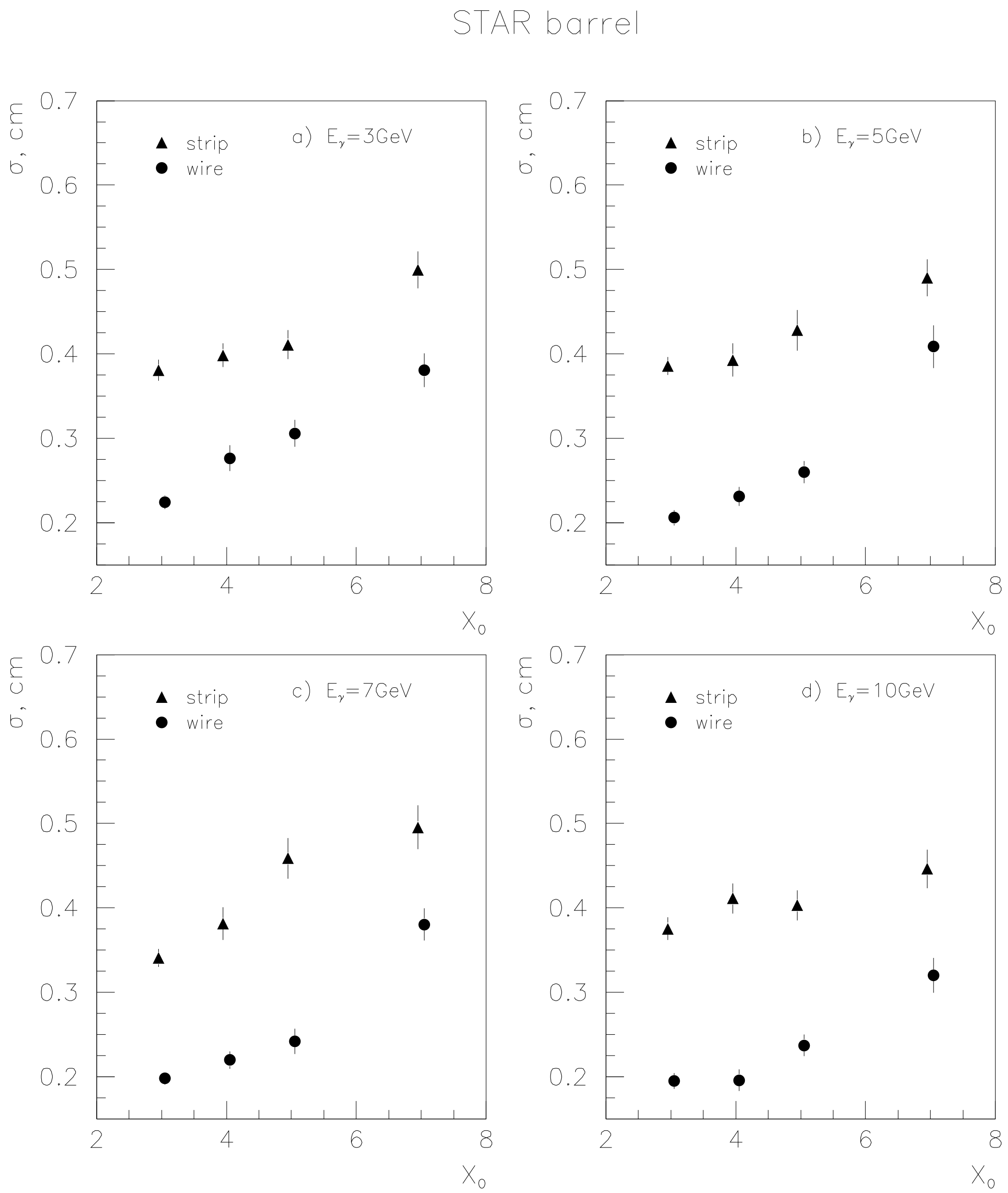

Figure 3: SMD position resolution for γ-quanta at various SMD locations in the EMC.

strip and Y_i is the position of the i-th anode wire; E_{tot} is the total energy deposition in the SMD. The free parameter W_0 has been varied within some range to achieve the best results for the position resolution as well as for the recognition of multiple overlapping γ-hits which is discussed later on in this paper. Among other things, parameter W_0 effectively sets the threshold, floating from shower to shower, for the energy deposition in each particular channel, $E_{min} = E_{tot} \cdot \exp(-W_0)$.

A typical resolution in the SMD is in the scale of few millimeters. The resolution is better for the shallow SMD positions compared to the deeper its locations. However, the spatial resolution is not the only parameter for the optimization of the SMD placement in the EMC. Other important characteristics such as γ and electron detection efficiencies, double-hit recognition, electron–hadron separation, etc must also be taken into account. The narrowing the SMD channel from 14 mm (strips) down to 7 mm (wires) gives the almost proportional improvement in the spatial resolution. However, this does not come "for free" but requires to double the number of the SMD channels from the defined in the project ~35–40k (barrel SMD only) to ~70–80k, and must also be weighted against the improvement of the EMC/SMD performance in general.

4 π^o/γ - Separation

In the simulations presented here, the effectiveness of the simple criteria for π^o/γ-separation based on the shower width in the SMD has been studied. These criteria were similar to those used in Refs.[10].

For each SMD shower, the "logarithmic weighted shower widths", $< R_x >$ and $< R_y >$, have been calculated:

$$< R_x >= \left[\frac{\sum_i W_i (X_i - X_c)^2}{\sum_i W_i} \right]^{1/2} ; \quad < R_y >= \left[\frac{\sum_i W_i (Y_i - Y_c)^2}{\sum_i W_i} \right]^{1/2} \qquad (2)$$

The meaning of parameters in Eqs. (2) is the same as in Eqs. (1) for the center of shower.

The single combined characteristic of the shower size, "mean weighted radius" $< R >$, which we used for π^0/γ-separation has been defined as

$$< R >= \sqrt{< R_x >^2 + < R_y >^2} \tag{3}$$

Typical $< R >$-distributions for the showers in the SMD originated from single photons and π^o-decays at three SMD locations are shown in Figs. 4–6. At low energy end, two peaks, for single-photon and for π^0s, are clearly seen. In this energy range, the background from π^0s under the single-γ peak is mainly due to the events with one photon of two lost because of the detection inefficiency in the SMD. This inefficiency, along with other factors, significantly depends on the floating threshold set by the choice of parameter W_0 (see Eqs.(1)). Therefore, setting the threshold at a feasibly lowest level is the key issue for catching as many as possible decays of low energy π^0s which is important to precisely evaluate the contribution of π^0s into the total photon production in the collisions of interest and, eventually, to estimate the yield of direct-γ with the acceptable accuracy.

At high energies, the distance in the SMD between two γ's from π^o-decays becomes smaller, resulting in that two showers usually overlap. As a consequence, the single-photon and π^0 separation at high energies is actually the problem of recognition and rejection of overlapping, presumably wider than single-hit clusters while keeping the efficiency to single photons, ϵ_γ, at a reasonably high level.

In this study, the $< R >$-cuts have been applied to separate single-γ and π^0 hits. These cuts along with the optimal values of parameter W_0 have been chosen individually for each energy and SMD location from the requirement of having $\epsilon_\gamma = 80\%$.

The results of simulations of "π^0 suppression power"[2] are shown in Figs. 7 and 8. One can observe that $< R >$-cut provides the highest suppression power for the SMD location at $\sim 5X_o$, and it works the best at the energies $\sim$3–10 GeV which overlap the range of interest for QGP search at RHIC through direct-γ yield measurements. Outside this energy interval, the suppression power of $< R >$-cut drops quite significantly. This means that the study of others, more sophisticated criteria is necessary to improve γ/π^0-separation at the both low and high ends of the energy spectrum of interest for the STAR experiment.

[2]Which is actually the π^0 hit's recognition efficiency, ϵ_{π^0}.

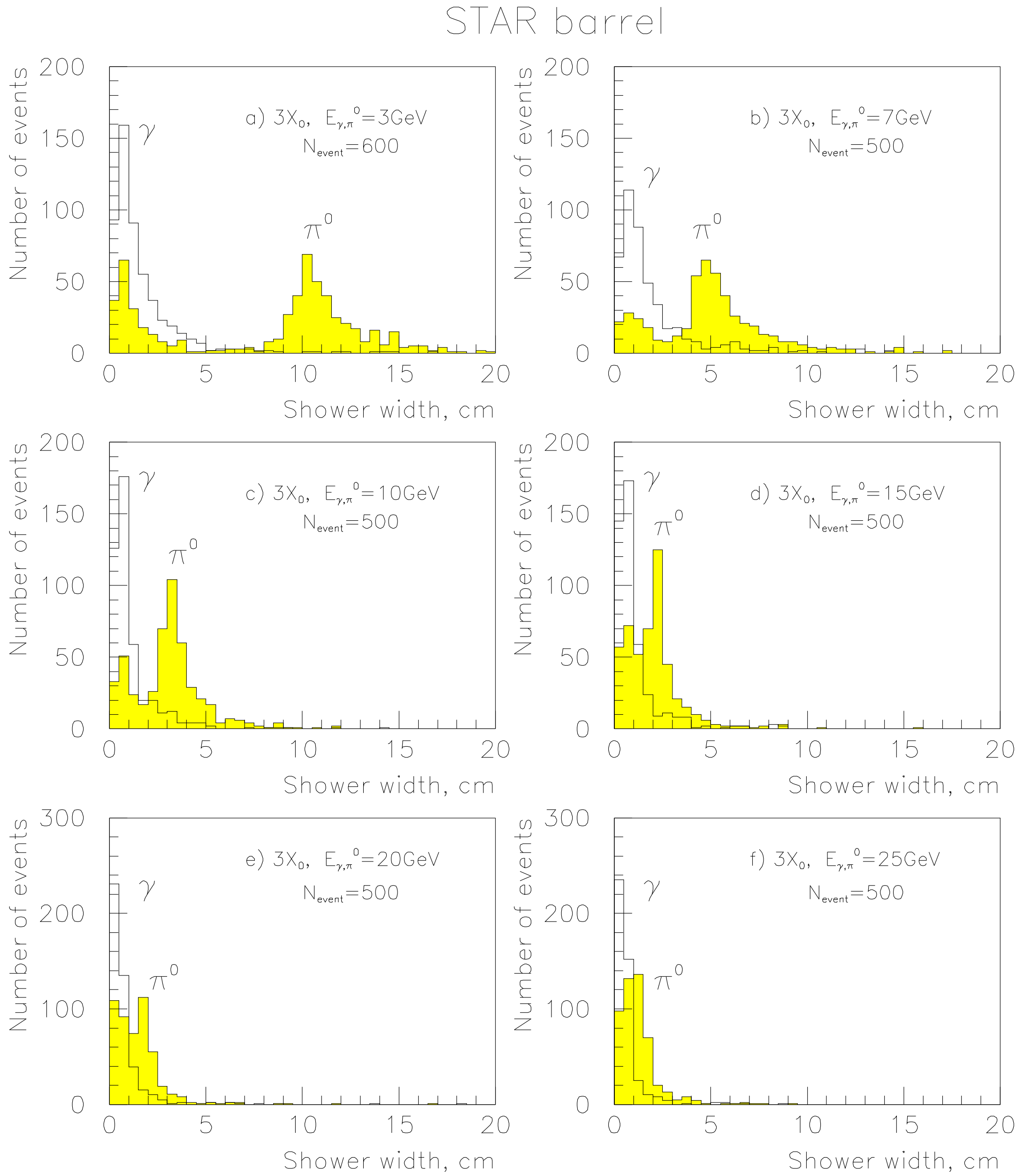

Figure 4: Typical distributions of the shower width, $< R >$, for clusters, originating from single-photons and π^o-decays, in the SMD located at $3X_o$.

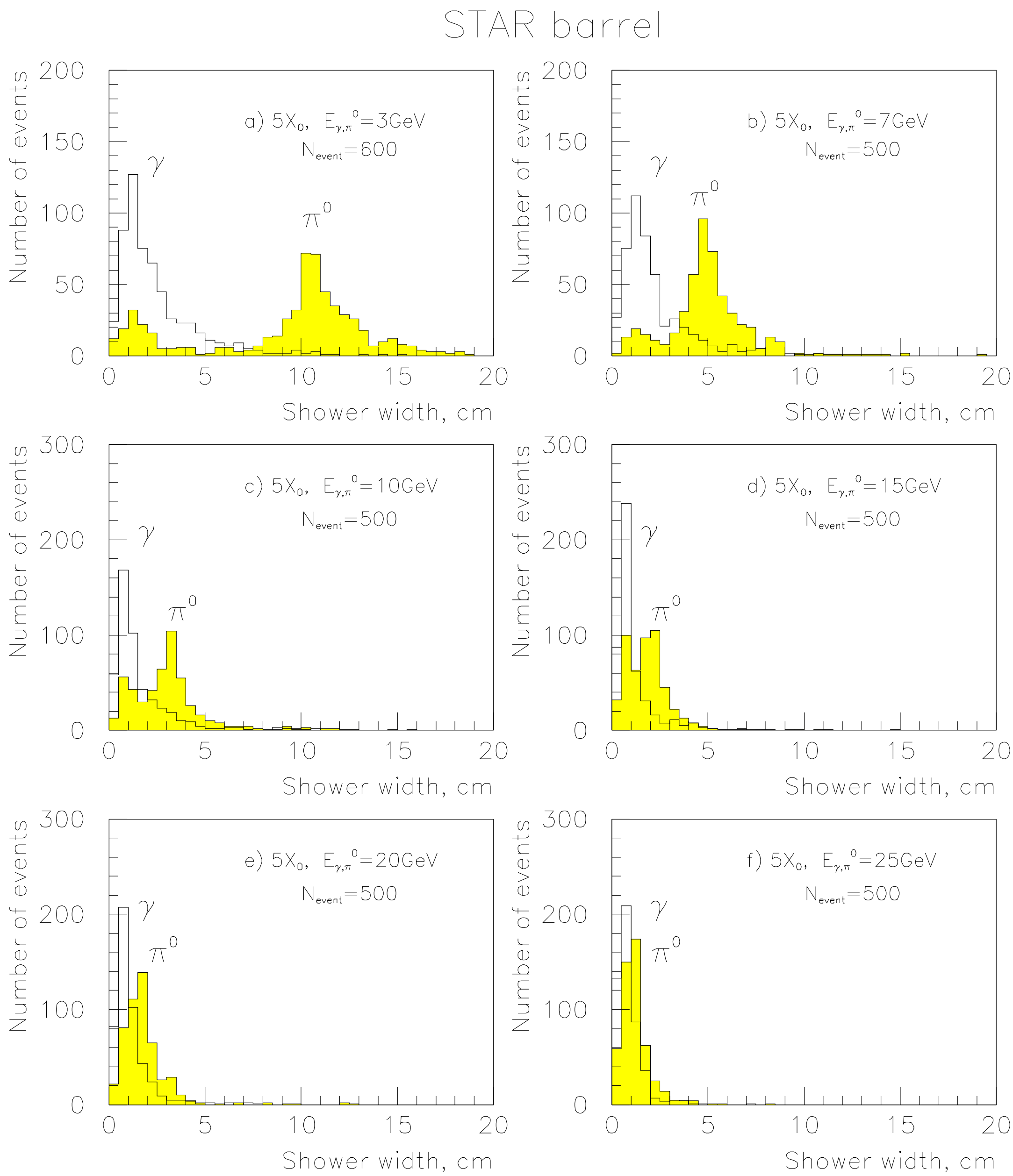

Figure 5: Same as in Fig.4 for the SMD located at $5X_o$.

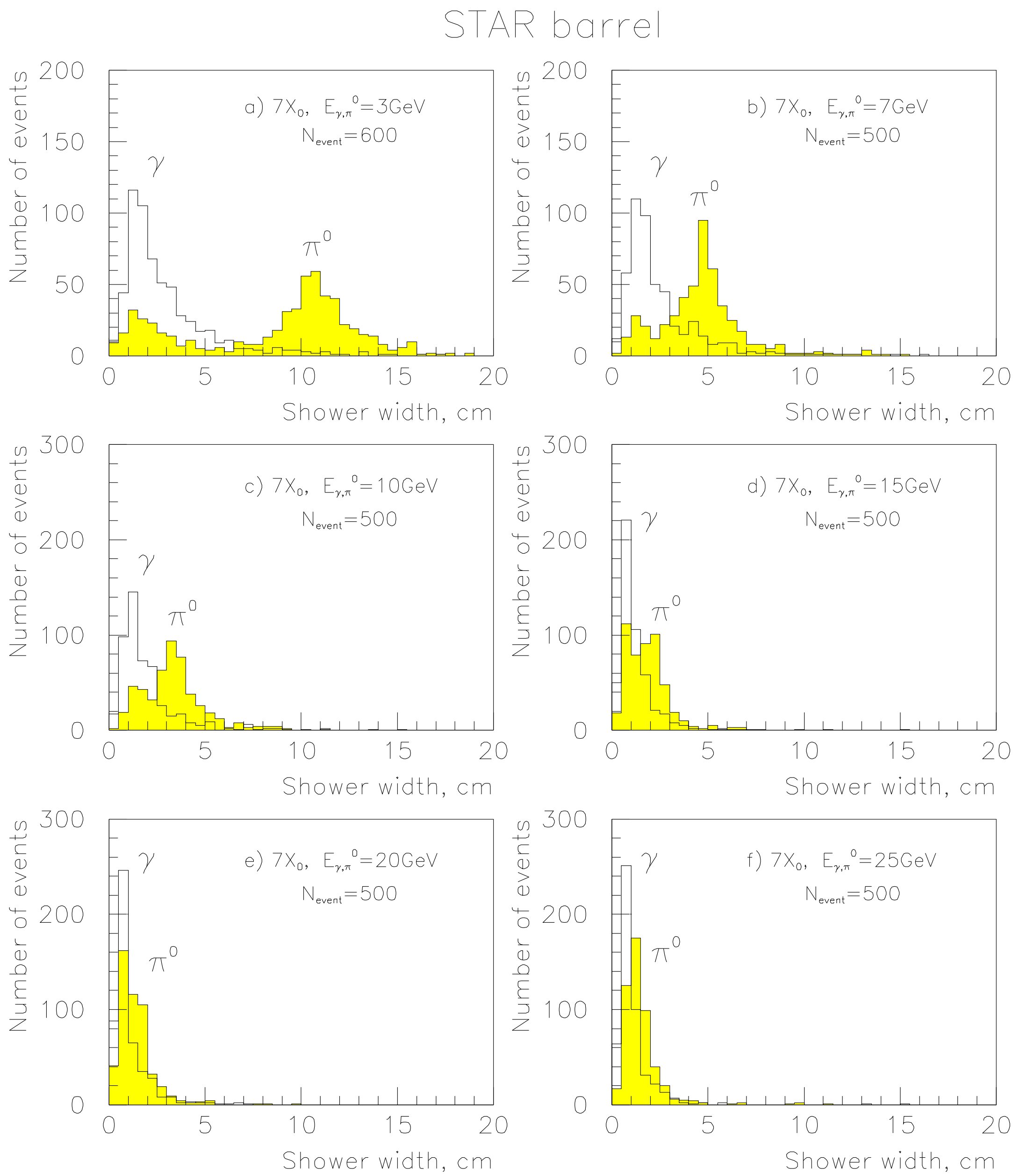

Figure 6: Same as in Fig.4 for the SMD located at $7X_o$.

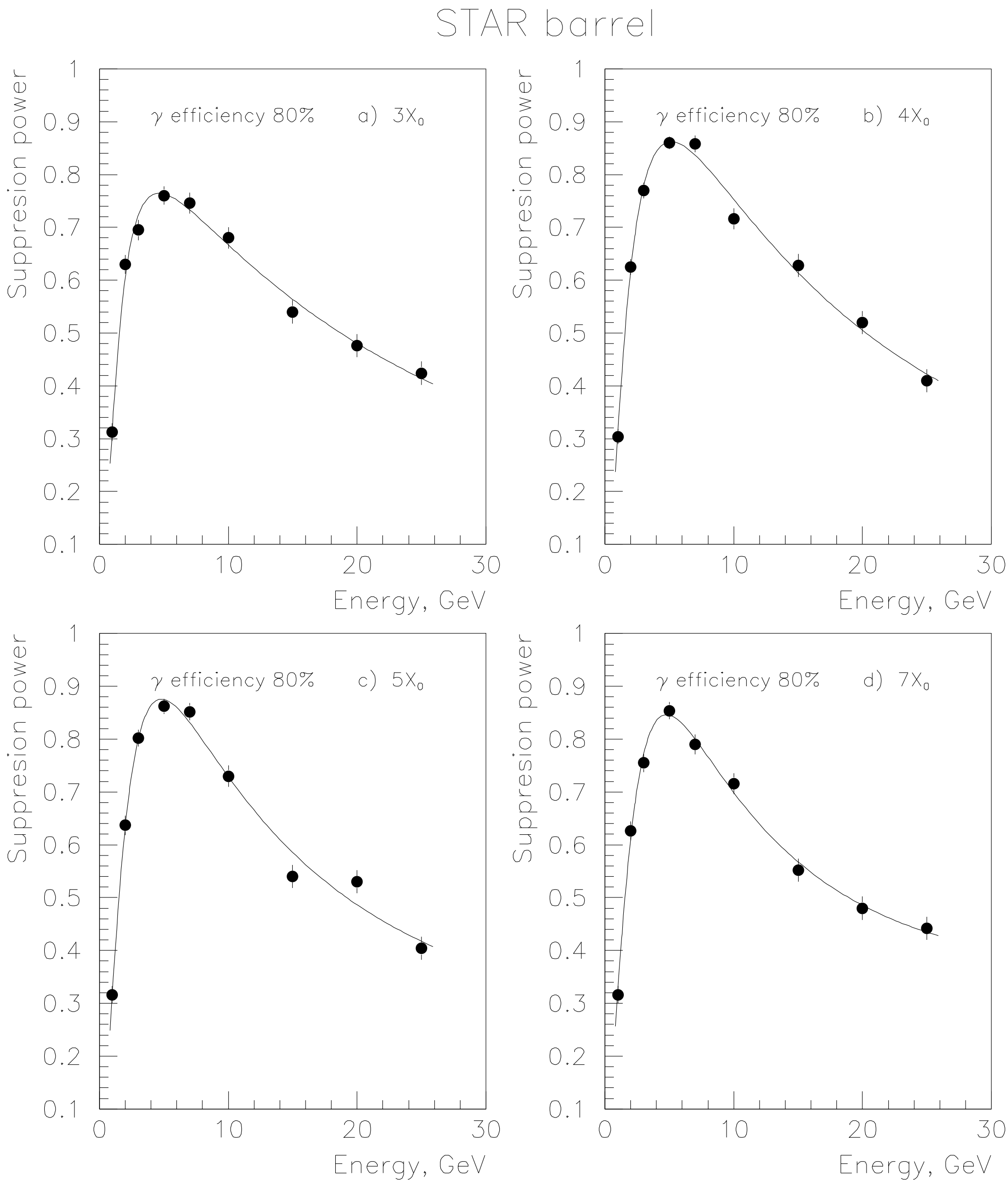

Figure 7: The simulated π^0 suppression power at 80% efficiency of single-γ detection for four SMD locations in the EMC stack.

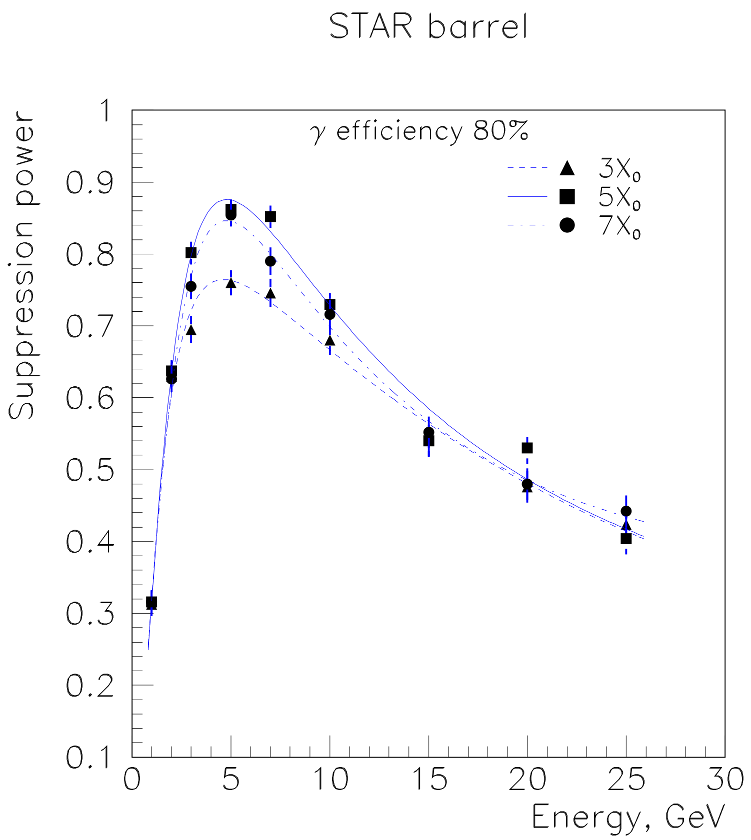

Figure 8: The comparison of π^0 suppression powers at 80% efficiency of single-γ detection for three SMD locations in the EMC stack.

The "strengthening coefficient" of the signal-to-background ratio, that is $\epsilon_\gamma/(1-\epsilon_{\pi^o})$, is the largest at the energies $\sim$3–7 GeV and, for the SMD location at $5X_o$, it reaches the value of $\simeq$4–6.5.

We have also tried using the other characteristic of clusters in the SMD to recognize single- and double-γ hits, the "inertia moment" ER^2 which contains the information about the showers size weighted with the energy deposition:

$$ER^2 = ER_x^2 + ER_y^2, \tag{4}$$

where $ER_x^2 = \sum_i E_i R_{xi}^2$ and $ER_y^2 = \sum_i E_i R_{yj}^2$ are the second moments for the strips and wires, respectively; $R_{xi} = X_i - X_c$ and $R_{yi} = Y_i - Y_c$. However, the simulations have shown that the criterion of "inertia moment" applied on top of $< R >$-cut does not provide a noticeable improvement of γ/π^0-separation in the SMD.

5 e/π - Separation

The hadron suppression coefficient, K_R, for the particles of the known momentum is defined here as a probability to misidentify a charged π-meson as an electron for 90% electron detection efficiency[3]. The $\sim 18X_o$ thick non-segmented EMC provides the suppression at the level of $K_R \simeq 0.01$–0.1 for the incident particle's energies from 2 to 30 GeV. The $< R >$-cut for the shower width in the SMD gives an additional factor of $\sim$2–3, resulting in the total suppression power of the EMC+SMD on the order of 0.003–0.06. The results of simulations for e/π-separation are presented in Fig.9. From these results, it also follows that the SMD position at $5X_o$ is more preferable than at $3X_o$.

6 Conclusion

Using the simplest method to distinguish single photons from $\pi^o \to 2\gamma$ decay, namely the shower width in the gaseous SMD, we have found that, in the wide energy range, the best results can be achieved for the SMD position close to $\sim 5X_o$ within the EMC stack. At this location for $E_\gamma \simeq 3$–7 GeV, the γ/π^o "signal-to-background" ratio can be improved by $\sim$4–6.5 times. We hope that by exploiting some other EMC and SMD features, these numbers can be improved.

[3]To avoid a potential confusion, we have to underline that the coefficient K_R as it is defined here is rather the characteristic of the EMC+SMD themselves which is usually measured in the beam tests [7] than the evaluation of the hadron suppression in the STAR detector. In the real setup, the particle momentum is never measured exactly. This will make the real hadron suppression power in STAR to differ, sometimes significantly, from that provided here. This is particularly true for high-P_T region where the momentum resolution in the STAR tracking system is considerably worse compared to the energy resolution in the EMC. The latter, in fact, was the only one of two resolutions which have been taken here into account to set the cuts for achieving 90% electron detection efficiency.

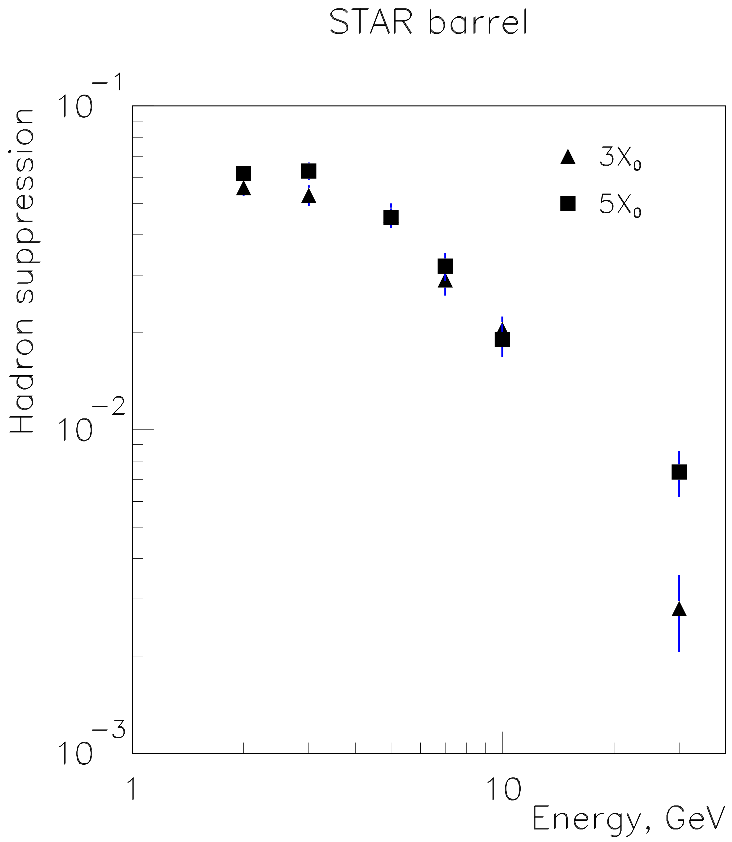

Figure 9: e/π-separation power vs energy of incident particles for two SMD locations in the EMC stack: at $3X_o$ and $5X_o$.

For example, at $P_T \leq$ 5–6 GeV/c, two photons from from π^0-decay will mostly strike different EMC towers of the size $\eta \times \varphi \simeq 0.05\times0.05$ each and even SMD patches of the size 0.1×0.1. In many cases, the energies and positions of both photons can be measured, and the invariant mass of the pair reconstructed. This provides the opportunity to evaluate the yield of low P_T π^0-mesons and, eventually, the yield of direct photons in the high combinatorial background of the high multiplicity heavy-ion collisions. The first simulation results, using this approach [11, 12], are quite encouraging although many important details of the photon shower's characteristics in the EMC and SMD have been omitted in these studies.

At the high energy end, more sophisticated algorithms for the recognition of single-γ and π^o-decays are to be explored (fit of shower shape, etc), including the possibility of using the power of neural networks (see, for example, Ref. [13]).

For the known charged particle momentum, the cuts on the energy deposition in the EMC around its mean value along with the cuts on the shower width in the SMD at $5X_o$ give the hadron suppression coefficient at the level of a few percents for the energies less than 5–10 GeV. For higher energies, the suppression power increases and, at 30 GeV, it reaches $\sim 3\times 10^{-3}$. For the entire energy range from 2 to 30 GeV, the deep SMD positioning at $5X_o$ provides the better hadron rejection compared to the location at $3X_o$.

Acknowledgments

It's our pleasure to thank B. V. Chujko who kindly provided us the measured shape of the electron shower in the SMD, and O. D. Tsai for the useful discussions.

References

[1] S. A. Akimenko et al. Nucl. Instr. and Meth. **A365** (1995) 92.

[2] Proposal on Spin Physics Using the RHIC Polarized Collider (RHIC Spin Collaboration), August 1992; Proposal Update, September 1993.

[3] C. P. Singh. Phys. Rev. **236** (1993) 147.

[4] Xin-Nian Wang et al. Preprint LBL-38455.

[5] P. K. Job et al. Nucl. Instr. and Meth. **A271** (1988) 442.

[6] L. Balka et al. Nucl. Instr. and Meth. **A267** (1988) 272.

[7] W. J. Llope (for the STAR-EMC Collaboration). Report to the "VI International Conference on Calorimetry in High Energy Physics", INFN, Frascati (Roma), Italy, June 8–14, 1996; Proceeding in Frascati Physics Series, Volume VI, Eds. A. Antonelli, S. Bianco, A. Calcaterra, F. L. Fabbri. pp.187–197.

[8] B. V. Chujko. Private Communication.

[9] T. C. Awes et al. Nucl. Instr. and Meth. **A311** (1992) 130.

[10] J. Grunhaus et al. Preprint TAUP-1976-92, Tel Aviv University, Tel-Aviv, Israel, 1992.

[11] T. M. Cormier. Report to the STAR Collaboration Meeting, August 1996, BNL (unpublished).

[12] T. J. LeCompte. STAR Note #251, July 1996.

[13] N. G. Minaev. Preprint IHEP 94–142, Protvino, 1994.